

## Thermal Expansivity of Chicken Feather Fiber Reinforced Epoxy Composites

Mingjiang Zhan, Richard P. Wool

Department of Chemical Engineering and Center for Composite Materials, University of Delaware, Newark, DE 19716

Correspondence to: R. P. Wool (E-mail: wool@udel.edu)

**ABSTRACT:** Thermal expansivity of chicken feather fibers (CFFs) was studied using thermomechanical analysis for composite applications. CFFs have negative coefficient of thermal expansion (CTE) values in the axial direction at different temperature due to its semicrystalline structure. CFFs have a positive CTE value in the radial direction. The CTE values of epoxy/CFF composites can be predicted by the rule of mixing. CTE values of epoxy/CFF composites in the in-plane direction at various fiber content and temperature have been fully studied and the results can be used in composite design. We can use CFFs in composite materials to control the overall CTE of the composites to reduce the CTE mismatch between the composites and other components. © 2012 Wiley Periodicals, Inc. *J. Appl. Polym. Sci.* 000: 000–000, 2012

**KEYWORDS:** natural fiber; chicken feather fiber; thermomechanical properties; coefficient of thermal expansion; biobased composite

Received 18 April 2012; accepted 4 June 2012; published online

**DOI:** 10.1002/app.38142

### INTRODUCTION

Fiber reinforced composite materials are used in a diverse range of industries, including boating, infrastructure, sporting goods, automotive, aircraft, and electronic packaging.<sup>1</sup> Many different properties are important for the different applications. Among them, the coefficient of thermal expansion (CTE) is of particular importance for composites used in electronic packaging applications, such as printed circuit boards (PCBs). In PCBs, composites with suitable CTE values are needed to reduce the mismatch in thermal expansion between the composite substrate and the copper foil.<sup>2</sup> Upon a temperature change, the rates of expansion of composites are not the same in different directions due to the anisotropic nature of the materials. Thermal expansion in the out-of-plane direction can affect the reliability of printed circuits. Thermal expansion in the in-plane direction is more important for the PCBs because the difference in thermal expansion between the composite substrate and the copper foil can cause thermal stress and thermal bending on the PCBs.<sup>3</sup> Thermal stress over time can fatigue the PCBs and ultimately cause failure due to separation of the copper foil from the composites or cracking of the foil.<sup>4</sup> For glass fiber reinforced composites used for PCBs, the CTE in out-of-plane direction is much larger than in-plane direction.<sup>5</sup>

Mechanical properties of chicken feather fibers (CFFs) have been studied<sup>6</sup> and CFFs have been used for different composite applications.<sup>7,8</sup> CFFs have promising dielectric properties and electrical resistivity, which is good for PCB packaging if

combined with suitable resins.<sup>9,10</sup> The previous study showed that CFFs had negative CTE values.<sup>11</sup> Its thermal expansivity has yet to be fully studied. CFFs are organic fibers; thus, we expect that they have similar thermal behavior as other organic fibers. For example, Kevlar fibers are synthetic aramid fibers and have a negative thermal expansion in the longitudinal direction.<sup>12,13</sup> In addition, some symmetric, balanced, angle-ply laminates of fiber reinforced plastics exhibiting negative CTE values in one of the in-plane principal directions have been studied.<sup>14</sup> In contrast, CFFs consist of short fibers with various lengths and diameters and its thermal expansivity has not been reported. The CTE values of randomly oriented CFFs composites and a mathematical model to predict CTE values are also of interest.

To reduce the dielectric constant of electronic materials, researchers developed porous materials to incorporate air.<sup>15</sup> However, the porous materials do not have enough mechanical strength and also increase CTE values. CFFs have hollow structure, low dielectric constant, and relatively high strength. PCB materials reinforced with CFFs will decrease the dielectric constant but do not bring thermal expansion problem. This unique virtue could be of great interest for the PCB industry.

Various techniques have been developed to obtain feather fibers and then use these fibers to make composites.<sup>16–18</sup> It was found that feather fibers can be extruded and can be processed at the same conditions as polyethylene. The good processability makes CFFs suitable for various applications.

Polymers for PCB applications have a broad range of glass transition temperature ( $T_g$ ) from 90 to 250°C.<sup>19</sup> Epoxy resins are widely used for PCBs. In this study, we used EPON 862 as a model polymer for PCB because it is a common epoxy with reasonable  $T_g$ . We fabricated composites from CFFs and EPON 862 epoxy resin. The CTE values of CFFs, epoxy, and the composites were investigated and compared with different models. We expected to establish a better understanding of the thermal expansivity of the CFFs composites for PCB applications.

## THEORETICAL

Thermal expansivity of a given composite material for various applications such as PCBs, has high sensitivity to thermal stress. The thermal expansivity of a composite can be predicted if the following are known: (a) the thermal expansivity of the constituent materials; (b) the orientation and the volume fraction of the constituent materials; and (c) the laws of the expansivity as a function of the constituents' properties and their respective proportions. The knowledge of such data and laws enables one to design a composite with specific thermal expansivity.

The CTE can be defined in different ways. In this study, the instantaneous linear thermal expansivity was used. Consider a sample with initial length  $L_0$  at temperature  $T_0$  (25°C in this study),  $L_1$  at  $T_1$ , and  $L_2$  at  $T_2$ , the instantaneous CTE ( $\alpha_I$ ) at temperature  $T_m$ , is calculated as follows:

$$\alpha_I = \frac{1}{L_0} \frac{L_2 - L_1}{T_2 - T_1} \quad (1a)$$

$$T_m = \frac{T_1 - T_2}{2} \quad (1b)$$

The simplest law for CTE of composites is the rule of mixing,<sup>2,20–22</sup> which can be expressed as:

$$\alpha_c = \alpha_f \varphi_f + \alpha_m (1 - \varphi_f) \quad (2)$$

where  $\alpha_c$ ,  $\alpha_f$ , and  $\alpha_m$  represent the CTE values of the composite, fiber, and matrix, respectively, and  $\varphi_f$  is the fiber volume fraction.

Turner's model<sup>21</sup> takes into account the mechanical interaction between the different materials in the composites. The derived CTE value is:

$$\alpha_c = \frac{(1 - \varphi_f)E_m\alpha_m + \varphi_f E_f \alpha_f}{(1 - \varphi_f)E_m + \varphi_f E_f} \quad (3)$$

where  $E_m$  and  $E_f$  are the bulk moduli of matrix and fibers, respectively.

Schapery developed equations to predict the lower and upper bound of the composites, which are related to the rule of mixing and the Turner's model.<sup>22</sup>

To predict overall properties for a two-dimensional (2D), randomly oriented or planar random composite, different models have been proposed.<sup>23–27</sup> Ng et al. used the transformation field analysis method and the volume-weighted averaging equations

to develop closed-form expressions of the overall CTE values for different fiber orientations.<sup>28</sup> The overall CTE for 2D randomly oriented fiber composites was derived as:

$$\gamma_{11} = \gamma_{22} = \frac{1}{2}(\alpha_{22} + \alpha_{33}) \quad (4a)$$

$$\gamma_{33} = \alpha_{11} \quad (4b)$$

where  $\gamma$  can be considered as the volume-weighted effective CTE,  $\alpha$  is the CTE of the constituent, subscripts 1 and 2 denote the in-plane directions, and 3 denotes the out-of-plane direction.

## EXPERIMENTAL

### Materials

Intact CFFs for single fiber thermal expansion tests were obtained from the Allen Laboratory at the University of Delaware. Single barbs were carefully removed from the rachides of CFFs. The optical and electronic scanning micrographs can be seen from the previous publication.<sup>6</sup>

CFFs for composites were provided by Featherfiber Corp. (Nixa, MO). This feather fiber is semicrystalline and has a diameter of about 5  $\mu\text{m}$ .<sup>29</sup> CFFs were dried in an oven at 50°C for at least 4 hours and then stored in a desiccator before use. EPON 862 epoxy resin (diglycidyl ether of bisphenol-F) and curing agent Epikure W were obtained from Hexion Specialty Chemicals, Inc. (Houston, TX).

### Sample Preparation

For composites of EPON 862/CFF, various amounts of CFFs (0%, 13, 27, 45, 49, 67 vol%) were mixed with EPON 862/Epikure W (weight ratio of EPON 862 to Epikure W was 100 to 26.4). The resin/fiber mixtures were degassed *in vacuo* for 5–10 min to remove air bubbles. The fiber/resin mixture was then spread onto a 200 mm  $\times$  200 mm rectangular mold which was subsequently closed and compressed using a hot press. The composites were cured at 120°C for 4 hr. The resulting composite panels were about 2 mm thick.

### Fiber Orientation

Fiber orientation analysis was performed using a Hitachi TM1000 tabletop scanning electron microscope (Hitachi High Technologies, Japan). Both top-view and cross-sectional view were examined. The composite surface was polished and the top-view was measured. The composite was also cut by a razor blade on the direction which is perpendicular to the polished surface and the cross-sectional view was measured using the scanning electron microscope.

### Thermomechanical Analysis (TMA)

A single fiber was mounted in a fiber clamping device. The thermal expansivity of the single feather fiber was measured using a TMA (Mettler-Toledo TMA/SDTA 841e, Greifensee, Switzerland) from 20 to 90°C at a heating rate of 2°C/min and with a preload of 0.01 N. Under such temperatures, feather fibers are still stable.<sup>30</sup> The dimension and the temperature of the sample were recorded by the TMA. Data were recorded every second or at 1/30°C intervals.

The thermal expansivity of the single feather fiber was also measured using a Nikon Eclipse E600POL microscope equipped

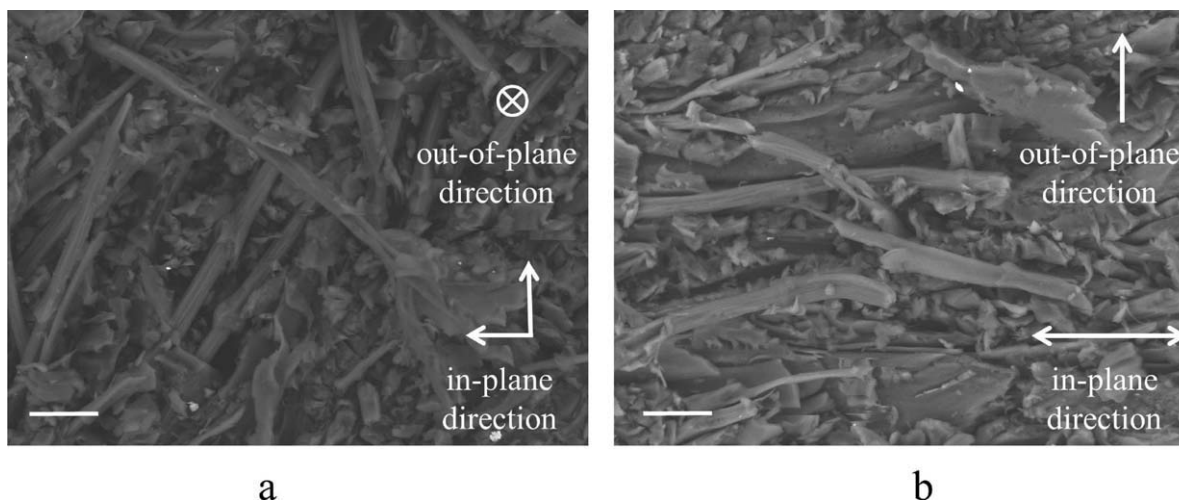


**Figure 1.** Fiber orientation of EPON/CFF composite. (a) top-view. CFFs oriented in the in-plane direction randomly. The out-of-plane direction is perpendicular to the paper surface. (b) cross-sectional view. Scale bars: 20  $\mu\text{m}$ .

with a hot stage and a high speed video camera from 25 to 125°C at every 5°C. The temperature was held at equilibrium for 10 min before the length of the fiber was recorded.

The thermal expansivity of EPON/CFF composites was measured using the TMA 841e equipped with a 3-mm ball-point quartz probe. Samples were randomly selected and cut from the molded composite panel. The measurement was performed from 20 to 90°C at a heating rate of 2°C/min and with a preload of 0.1 N. A round quartz disk was used between the probe and the sample to evenly distribute the preload to the sample. For each fiber volume fraction, two specimens were measured. Data were recorded every second or at 1/30°C intervals.

The CTE values were calculated by the first-order derivative of the length-temperature curves.

## RESULTS AND DISCUSSION

### Fiber Orientation

The orientation of the fibers is shown in Figure 1. From the top-view [Figure 1(a)] we can see that CFFs oriented in the

in-plane direction randomly. From the cross-sectional view [Figure 1(b)] we can also see that most fibers were oriented in the in-plane direction. Both directions confirm that the 2D random fiber orientation assumption is valid. However, a few fibers did not align perfectly on the in-plane direction, which suggests that errors may exist if we use the 2D random fiber orientation assumption.

### Longitudinal (Axial) CTE of Single CFF and CTE of the Neat Epoxy Resin

TMA measures very slight dimensional changes of a sample as a function of temperature. Figure 2(a) shows the length change of neat EPON 862 epoxy polymer and a CFF at elevated temperatures. The length of epoxy increased almost linearly from 25 to 90°C. In contrast, the length of the CFF decreased along its longitudinal direction as the temperature increased.

The dimensional change of a material is affected by atomic bonding, molecular structure, and molecular assembly.<sup>31</sup> When the temperature increases, the thermal energy of the material also increases, which leads to increasing atomic movement. A

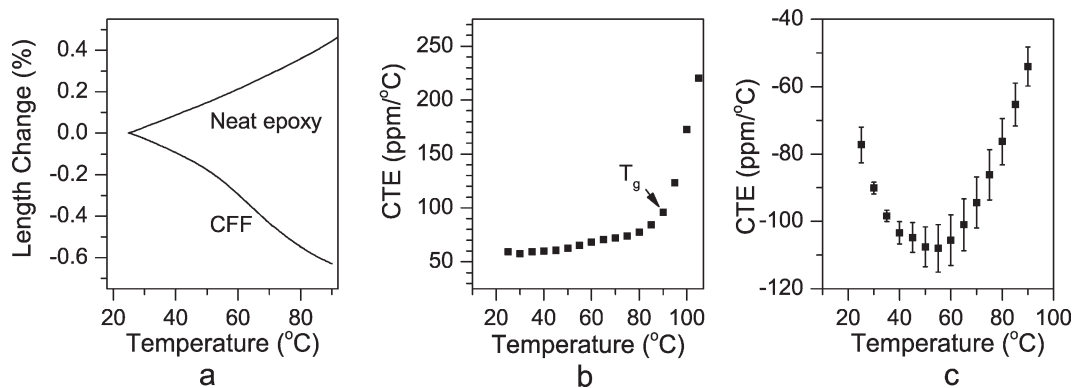


**Figure 2.** Thermomechanical properties of EPON 862 and CFFs. (a) The length (normalized to the initial lengths at 25°C) change of EPON 862 epoxy polymer and chicken feather fiber at elevated temperatures. (b) The coefficients of thermal expansion of EPON 862 epoxy as a function of temperature. (c) The coefficients of thermal expansion of CFFs in the longitudinal direction as a function of temperature. CFFs had negative CTE values in the whole temperature range. The error bars are the standard deviation.

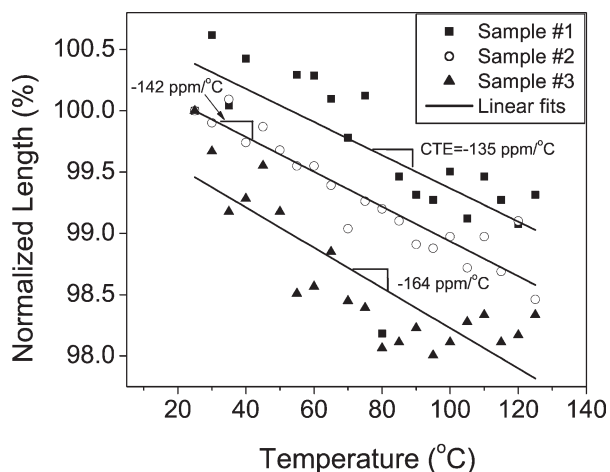


**Figure 3.** The normalized length of feather fibers at elevated temperature from 25 to 125°C measured by an optical microscope equipped with a hot stage. The lines are linear fits of three different samples.

low atomic anharmonic bonding energy would show a higher dimensional change due to an increasing interatomic distance.<sup>31</sup> The increasing atomic movement causes the expansion of the EPON resin. CFFs are composed of keratin proteins with  $\alpha$ -helix and  $\beta$ -sheet structures, and thus, have a crystalline structure.<sup>32,33</sup> The inherent anisotropy of bonding along the protein chains causes the contraction of these highly ordered polymers upon heating, which is clearly seen in Figure 2(a). The thermal contraction also occurs in other organic fibers in the axial direction, such as aramid fibers<sup>12,34</sup> and polyethylene fibers.<sup>35</sup>

The CTE values of neat epoxy are shown in Figure 2(b). The CTE values of the epoxy resin can be divided into two segments: below and above its  $T_g$ . The CTE values remained constant or increased slightly at temperatures below its  $T_g$  and then increased dramatically above  $T_g$  because of the free movement of molecular segments above  $T_g$ .

We are mainly interested in the CTE values at the temperature below  $T_g$  because most polymers for PCBs are used below their glass transition temperature. Our discussion will focus on the temperatures below 80°C in the following sections.

Figure 2(c) shows the CTE of CFFs in the longitudinal direction. CFFs had negative CTE values in the whole temperature range. The CTE decreased initially until the temperature reached about 50°C and then increased. Rojstaczer et al. studied the CTE of aramid fibers and found that the CTE of aramid fibers also had a nonlinear trend and decreased with temperature.<sup>12</sup>

The orientation of the molecules causes significant anisotropy in the linear thermal expansion of polymers.<sup>36–39</sup> Kobayashi and Keller suggested that in the case of single crystal polyethylene, the shrinkage of the fiber with temperature was attributed to the increased rotation around C–C bonds on the backbone, leading to the twist of planar zig-zag.<sup>35</sup> Choy et al. studied the thermal expansion of a series of polymers with different crystallinity<sup>39</sup> and they proposed that an oriented polymer was composed of four phases: the crystallites, the amorphous region (the

floating chains attached to a crystalline block), intercrystalline bridges, and tie-molecules (connecting one crystalline block to another). For polymers with high crystallinity, the negative thermal expansion is mostly due to the contraction of the crystalline bridges. For low crystalline polymers it is mainly because of the rubber-elastic effect of the tie-molecule which produces the overall contraction in fiber axial direction. Choy et al. also observed a sharp decrease in CTE when the fibers pass the transition (either glass transition or subglass transition) temperature,<sup>39</sup> which suggests that CFFs might also have an amorphous transition at a temperature below 50°C. However, the exact reason why the CTE values of CFFs showed a minimum at about 50°C is still not confirmed.

To visibly observe the interesting thermal contraction behavior, the dimensional change of the fibers was also recorded by an optical microscope with a digital camera. Figure 3 shows the normalized length with respect to  $L_0$  [see eq. (1)] of feather fibers at different temperatures measured by a microscope equipped with a hot stage. In general, the length of the fiber decreased with temperature, indicating thermal contraction. Unlike in the TMA, the fibers on the hot stage had free ends; thus, the fibers could contract and curl. Due to the curling, the CTE values measured by optical microscopy (about  $-147$  ppm/°C) were lower than the values obtained by TMA (from  $-55$  ppm/°C to  $-110$  ppm/°C). For this reason, the CTE values obtained from the microscope were not used for the rest of the discussion. However, the visible evidence has verified the thermal contraction of feather fibers in the longitudinal direction.

#### Extrapolated Transverse (Radial) CTE of a Single CFF

It is important to know the radial CTE of the CFFs for further analysis on the CTE values of the composites. Unfortunately, it is not feasible to directly measure the radial CTE due to its

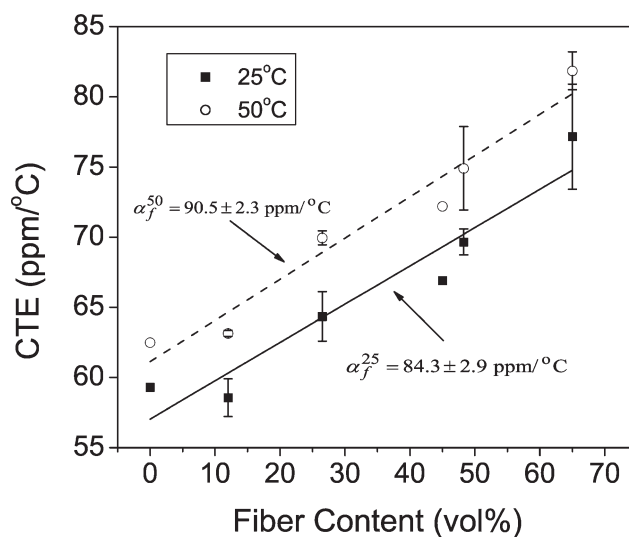


**Figure 4.** The coefficients of thermal expansion of the out-of-plane direction of the EPON/CFF composites as a function of fiber volume fraction at 25 and 50°C. The CTEs were fitted by rule of mixing equation to obtain radial CTE of the chicken feather fibers ( $\alpha_f^T$ ). The error bars are the standard deviation.

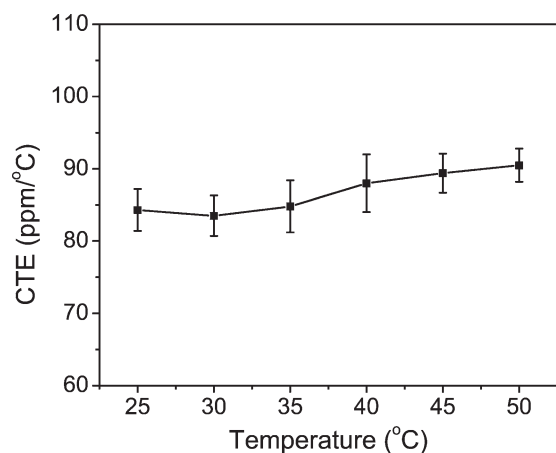


**Figure 5.** The radial CTEs of chicken feather fibers as a function of temperature. The error bars are the standard deviation.

small diameter. Instead, the CTE was indirectly measured, by extrapolating the transverse expansivity of the EPON/CFF composites. The assumption was that the fibers in the EPON/CFF composites were fully 2D oriented; that is, the axial direction of fibers was perfectly parallel to the in-plane direction of the composites. To determine the radial CTE of the feather fiber, the rule of mixing equation was used.<sup>21,22</sup>

The CTE values of the out-of-plane (transverse) direction of the EPON/CFF composites increased linearly with increasing fiber volume fraction within the temperature range of 25–50°C (Figure 4), which indicates that the rule of mixing is suitable to retrieve the radial CTE of the feather fibers. The experimental data was fitted by a linear equation (rule of mixing) to obtain the radial CTE of the CFFs ( $\alpha_f^T$ ). Figure 4 shows CTE values at 25 and 50°C only; however, the same method can be applied to all temperatures. The obtained radial CTE values of CFFs are shown in Figure 5. The variation shown in the Figure is due to the heterogeneity of feather fibers. The effects of the heterogeneity on feather fiber properties were discussed previously.<sup>6</sup> If the standard deviations are considered, there was no significant difference among CTE values at different temperatures. The aver-

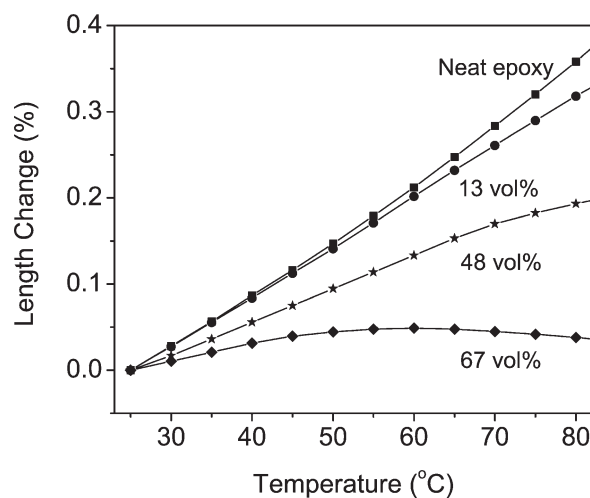


**Figure 6.** The length change of EPON/CFF composites in the in-plane direction as a function of temperature at various fiber loadings. The length was normalized to the initial length at 25°C.

age value of  $86.8 \pm 2.9$  ppm/°C was used for further analysis. Aramid fiber, another organic fiber, has an  $\alpha_f^T$  value of 66.3 ppm/°C,<sup>12</sup> which is similar to CFFs.

#### Longitudinal (In-plane Direction) CTE of EPON/CFF Composites

The dimensional change of the composite in the in-plane direction as a function of temperature is shown in Figure 6. In general, composites expanded as the temperature increased. The length change decreased with increasing fiber content because CFFs has a negative CTE value in the axial direction. For the composite with 67 vol % CFFs, the length increased slightly at ambient temperature and then reached maximum at around 60°C because with enough CFFs, the thermal expansion of the matrix materials is compensated by the thermal contraction of CFFs.

On the basis of the fully 2D orientation assumption, the contribution of CTE in the in-plane direction from CFFs was a

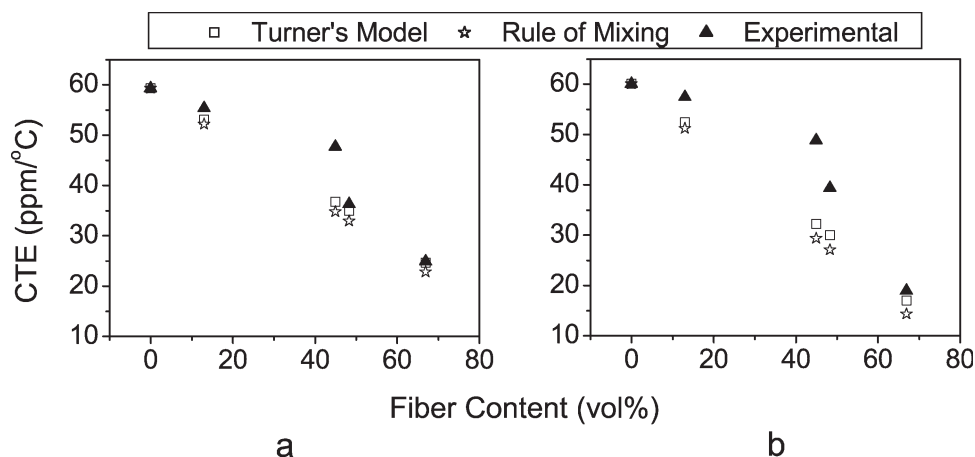


**Figure 7.** Experimental and theoretical in-plane CTEs of the EPON/CFF composites as a function of fiber content at different temperatures. (a) 25°C and (b) 40°C.

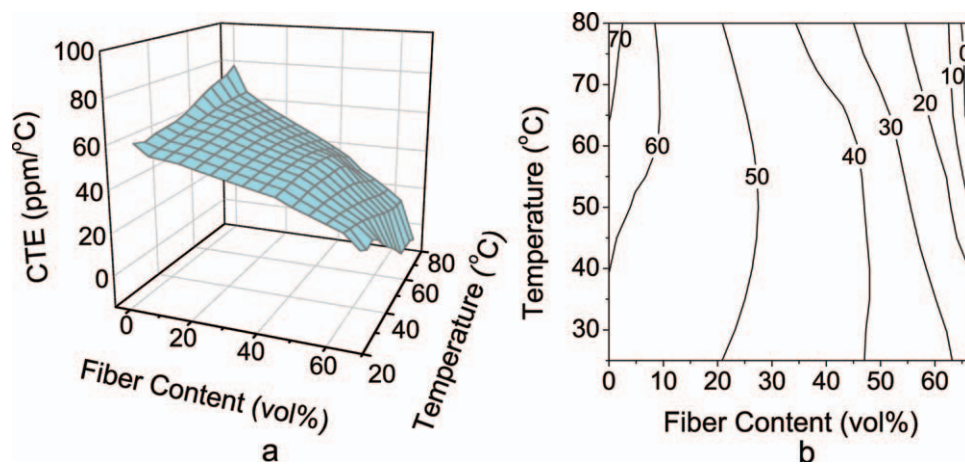


**Figure 8.** 3D plots of the CTE of EPON/CFF composites in the in-plane direction as a function of fiber content and temperature. (a) surface plot and (b) contour plot. [Color figure can be viewed in the online issue, which is available at [wileyonlinelibrary.com](http://wileyonlinelibrary.com).]

combination of the axial and radial CTE values of CFFs. Following Ng et al.,<sup>28</sup> eq. (4a) was used to calculate the effective CTE of the CFFs. The modulus values of EPON epoxy and CFFs were obtained from literature<sup>6,30</sup> and used in eq. (3) to calculate the CTE values of the composites. The theoretical and experimental in-plane CTE values of the composites as a function of fiber content at different temperatures are shown in Figure 7. The calculated CTE values by Turner's model and the rule of mixing were very similar because the modulus of EPON epoxy and the feather fibers are very close. In general, the experimental results showed good agreement with the theoretical predictions. The CFFs may not fully lie on the in-plane direction during composite fabrication (Figure 1). Hence, the assumption of 2D orientation causes errors, which explains some disagreement between the models and the experimental data. The heterogeneity of the fibers may cause additional errors.<sup>6</sup>

Given the CTE values of EPON/CFFs composites in the in-plane direction at various fiber content and temperatures, a three-dimensional (3D) surface plot of CTE values obtained from the TMA is shown in Figure 8(a) and the corresponding contour plot is also shown in Figure 8(b). From the plots, the CTE value of the composites at a given fiber content and temperature can be determined, which is very helpful for designing a composite with desirable CTE values. For example, the CTE of copper foil is about 18 ppm/°C. According to the 3D surface plot and the contour plot, one is able to design a composite for PCB application with certain fiber content, which consequently has a CTE close to that of the copper foil. Hence, the design will reduce the thermal stress of the PCBs and improve its life-time.

## CONCLUSIONS

CFFs have negative longitudinal CTE values that are temperature dependent, due to its crystalline structures of  $\alpha$ -helix and  $\beta$ -sheet. The inherent anisotropy of bonding along the protein chains causes the contraction of CFFs upon heating. CFFs have a positive transverse CTE value like other organic fibers. The CTE values of feather fiber composites vary as a function of volume fraction and temperature and can be predicted by the rule

of mixing. We can use the feather fibers in composite materials to reduce the overall CTE values to minimize or diminish the CTE mismatch between the composites and other components, such as the copper foil used in PCBs. We have fully estimated CTE values of EPON/CFF composites in the in-plane direction as a function of fiber content and temperature, which can help in composite design.

CFFs have diameters and lengths that vary greatly. In addition, the complete 2D orientation of fibers is approximate. Hence, additional testing and analysis are necessary to study the effects of the fiber orientation and fiber aspect ratio on the overall CTE values of the composites.

## ACKNOWLEDGMENTS

The authors thank Mr. Bo Peng and Dr. Linbo Wu at Zhejiang University for the fiber length measurement under microscope. They thank Featherfiber Corp. for providing feather fibers and Hexion Specialty Chemicals for supplying the EPON 862 epoxy and curing agent. They also gratefully acknowledge financial support from the United States Department of Agriculture-Cooperative State Research, Education, and Extension Service-National Research Initiative (USDA-CSREES-NRI), contract grant number 2005-35504-16137.

## REFERENCES

1. Mazumdar, S. K. *Composites Manufacturing: Materials, Product, and Process Engineering*; CRC Press: Boca Raton, 2002.
2. Tani, J.; Kimura, H.; Hirota, K.; Kido, H. *J. Appl. Polym. Sci.* **2007**, *106*, 3343.
3. Ishikawa, T.; Chou, T. W. *J. Compos. Mater.* **1983**, *17*, 92.
4. Kelley, E. J. In *Printed Circuits Handbook*; Coombs, C. F., Ed.; McGraw-Hill: New York, 2007.
5. La Carrubba, V.; Butters, M.; Zoetelief, W. *Polym. Bull.* **2008**, *59*, 813.
6. Zhan, M.; Wool, R. P. *Polym. Compos.* **2011**, *32*, 937.

7. Cheng, S.; Lau, K. T.; Liu, T.; Zhao, Y. Q.; Lam, P. M.; Yin, Y. S., *Compos. Part B: Eng.* **2009**, *40*, 650.
8. Huda, S.; Yang, Y. Q. *Compos. Sci. Technol.* **2008**, *68*, 790.
9. Zhan, M.; Wool, R. P.; Xiao, J. Q. *Compos. Part A: Appl. Sci. Manuf.* **2011**, *42*, 229.
10. Zhan, M.; Wool, R. P. *J. Appl. Polym. Sci.* **2010**, *118*, 3274.
11. Zhan, M.; Wool, R. P. Annual American Physical Society Meeting, Denver, CO, March 5–9, **2007**.
12. Rojstaczer, S.; Cohn, D.; Marom, G. *J. Mater. Sci. Lett.* **1985**, *4*, 1233.
13. Anonymous., Kevlar Aramid Fiber-Technical Guide; Retrieved on August 8th, 2011 from Available at [http://www2.dupont.com/Kevlar/en\\_US/tech\\_info/index.html](http://www2.dupont.com/Kevlar/en_US/tech_info/index.html).
14. Ito, T.; Suganuma, T.; Wakashima, K. *J. Mater. Sci. Lett.* **1999**, *18*, 1363.
15. Morgen, M.; Ryan, E. T.; Zhao, J. H.; Hu, C. A.; Cho, T. H.; Ho, P. S. *JOM-J. Min. Met. Mat. S.* **1999**, *51*, 37.
16. Gassner, G., III; Schmidt, W. F.; Line, M. J.; Thomas, C. G.; Waters, R. M. U.S. Patent 5,705,030, **1998**.
17. Barone, J. R.; Schmidt, W. F.; Gregoire, N. T. *J. Appl. Polym. Sci.* **2006**, *100*, 1432.
18. Barone, J. R.; Schmidt, W. F.; Liebner, C. F. E. *Compos. Sci. Technol.* **2005**, *65*, 683.
19. IPC, IPC 4101B—Specification for Base Materials for Rigid and Multilayer Printed Boards, **2002**.
20. Orrhede, M.; Tolani, R.; Salama, K. *Res. Nondestruct. Eval.* **1996**, *8*, 23.
21. Turner, P. S. *J. Res. Nat. Bur. Stand.* **1946**, *37*, 239.
22. Schapery, R. A. *J. Compos. Mater.* **1968**, *2*, 380.
23. Chamis, C. C.; Sendeckyj, G. P. *J. Compos. Mater.* **1968**, *2*, 332.
24. Christensen, R. M. *Int. J. Solids. Struct.* **1976**, *12*, 537.
25. Craft, W. J.; Christensen, R. M. *J. Compos. Mater.* **1981**, *15*, 2.
26. Wakashima, K.; Otsuka, M.; Umekawa, S. *J. Compos. Mater.* **1974**, *8*, 391.
27. Pettermann, H. E.; Bohm, H. J.; Rammerstorfer, F. G. *Compos. Part B: Eng.* **1997**, *28*, 253.
28. Ng, E. T. Y.; Wood, G. M.; Suleman, A. *J. Compos. Mater.* **2006**, *40*, 397.
29. Barone, J. R.; Schmidt, W. F. *Compos. Sci. Technol.* **2005**, *65*, 173.
30. Zhan, M. Bio-based composites from soybean oil resins and feather fibers for electronic applications, Ph.D. Dissertation, **2010**, University of Delaware, Newark, DE.
31. Wang, S. R.; Liang, Z. Y.; Gonnet, P.; Liao, Y. H.; Wang, B.; Zhang, C. *Adv. Funct. Mater.* **2007**, *17*, 87.
32. Fraser, R. D. B.; MacRae, T. P. Symposia of the Society for Experimental Biology Number XXXIV: The Mechanical Properties of Biological Materials, **1980**, p 211.
33. Fraser, R. D. B.; Macrae, T. P.; Parry, D. A. D.; Suzuki, E. *Polymer* **1971**, *12*, 35.
34. Strife, J. R.; Prewo, K. M. *J. Compos. Mater.* **1979**, *13*, 264.
35. Kobayashi, Y.; Keller, A. *Polymer* **1970**, *11*, 114.
36. Choy, C. L.; Chen, F. C.; Ong, E. L. *Polymer* **1979**, *20*, 1191.
37. Porter, R. S.; Weeks, N. E.; Capiati, N. J.; Krzewski, R. J. *J. Therm. Anal.* **1975**, *8*, 547.
38. Buckley, C. P.; Mccrum, N. G., *J. Mater. Sci.* **1973**, *8*, 1123.
39. Choy, C. L.; Chen, F. C.; Young, K. *J. Polym. Sci. Polym. Phys.* **1981**, *19*, 335.